

# A DC Voltage Control Strategy for MMC MTDC Grids incorporating Multiple Master Stations

C. E. Spallarossa  
T. C. Green  
Imperial College London  
London, UK  
[claudia.spallarossa10@ic.ac.uk](mailto:claudia.spallarossa10@ic.ac.uk)

Chang Lin  
Xueguang Wu  
State Grid Smart Grid Research Institute, SGCC  
Beijing, China  
[linchang@sgri.sgcc.com.cn](mailto:linchang@sgri.sgcc.com.cn)

**Abstract**—One of the responses to the increasing penetration of renewable energies along with the growth in electricity demand is the interest in the construction of multi-terminal DC grids (MTDC), as mean to connect onshore AC systems with remotely located offshore wind energy sources. This paper investigates the current methodologies for MTDC control stating their limitations for severe contingency conditions and proposes a control strategy able to ensure grid reliability and voltage stability in the case of a sudden outage of the converter station controlled in Vdc-Q. This strategy, acting on the Vdc reference signal, allows the presence of multiple master converters in the DC grid. A five-terminal DC scheme, which connects onshore AC systems with offshore wind farms, has been developed in RT-Lab Simulator. Each sub-station (terminal) is equipped with a modular multilevel converter (MMC). The converters are either Vdc-Q controlled (master stations) or are P-Q (with droop control) or Vac-frequency regulated. The dynamic response of the system is observed after a converter outage to assess the validity of the proposed DC voltage control strategy.

**Index Terms**—MMC, HVDC, MTDC, Droop Control, Voltage Stability.

## I. INTRODUCTION

The rapid increase of energy demand in combination with the significant penetration of renewable energy sources and the carbon emission reduction targets are forcing existing electricity networks to work closer to their operational limits. Consequently, the reinforcement of the existing power systems is becoming urgent. In the European scenario the construction of an overlay Super Grid represents a valuable solution [1], [2]. In this context the development of multi-terminal DC grids (MTDC) to exploit and connect remotely located offshore wind energy resources to onshore AC systems is an essential step towards the creation of such a Super Grid. Other countries are experiencing a similar situation; in China the growing wind penetration is leading to the broad diffusion of MTDC networks. One example is the “Zhoushan Project”, a five terminal DC scheme which includes both offshore wind and onshore AC systems [3], this

could be considered as a reduced scale representation of the future North Sea DC grid.

In this paper a MTDC model consisting of five terminals is used as a case study, the scheme is similar to the Chinese “Zhoushan Project” in terms of technologies implemented. The DC grid connects both onshore AC systems and offshore wind farms, modeled as Doubly Fed Induction Generators (DFIGs). The converter substations are equipped with Voltage Source Converters (VSCs) supporting modular multilevel topology. The VSC is recognized to be the best option for the MTDC technology thanks to its technical characteristics (independent control of active and reactive power, black start capability, lower losses and high reliability) [4]. Moreover the development of Modular Multilevel Converters (MMC) has enhanced the performance of VSCs. The MMC topology enables reduced power losses due to lower switching frequency, elimination of filter requirements, easy scalability to higher voltages and increased reliability thanks to the high number of sub-modules [5].

In the literature, the control strategies for MTDC grids have been classified as “Constant Vdc Control” (normally a master and slave scheme) and “P-Vdc Droop Control” (normally a peer-to-peer scheme) [6]. In the first scheme the reliability of the whole DC grid is jeopardized by an outage occurring at the master converter (a slack bus in terms of the DC network), as this is the only converter which can regulate its power flow to balance for Vdc variations. The second scheme enhances grid reliability by allowing all the terminals to participate to the power sharing and to the voltage regulation (through P against Vdc droop control) [6]. In spite of the good power balancing, this strategy does not ensure close regulation of Vdc for high loading conditions. In the case of an outage at one converter the dc voltage is observed to exceed the nominal limits (+/- 5%). On the other hand, the use of multiple master converters to provide control will potentially lead to conflicts. A new approach is presented here that ensures the correct power burden sharing along with voltage stability without the aid of communication links. The

MTDC scheme is equipped with two master (or slack) converters, whose Vdc control loops have been modified in order to avoid conflicts and keep the dc voltage within the limits in both steady state dynamic conditions.

The paper consists of five further sections. First the description of the MMC modeling is provided. Secondly the MTDC control strategy is illustrated; particular attention is dedicated to the implementation of P-Vdc droop and modified Vdc controls in slave and master converters respectively. The case study, describing the platform used to investigate the dynamic performance of the MTDC, is outlined in Section IV. Time-domain simulations are presented and the outcomes explained in the following section. Finally, some conclusions are drawn in Section VI.

## II. MMC MODELING

This section describes the structure and the control of the modular multilevel converter used in the MTDC grid.

### A. MMC Structure

A modular multilevel converter consists of three phase units, which are composed by an upper and a lower arm. A variable number of sub-modules (SMs), according to the converter rating required, are connected in series to form each arm. Every SM contains two pair of switches (IGBT and diode), and a capacitor [7]. The large number of SMs per arm reduces the voltage rating per module and the harmonic content of the output waveform improving the power quality [5]. The MMC has been modeled using the Nested Fast and Simultaneous Solution procedure as described in [8]. This approach reduces the computational time for electromagnetic transient simulations (EMT) and proposes an accurate model for every SM, being therefore able to represent the behavior of the system in case of sub-module failure.

### B. MMC Control

The control strategy of an MMC consists of several cascaded controllers. It can be divided in an upper level control (outer and inner controller) and lower level control (capacitor voltage balance and circulating current suppression control) [5] as shown in Fig. 1. In the upper level control the classical vector control strategy is applied. Through the inner control the current is decoupled in the synchronous reference frame (d-q). The two outer controllers are in charge of controlling P, Vdc and Q, Vac acting on d and q current reference respectively [9]. In the lower level control, the action of circulating current suppression control (CCSC) prevents arm currents distortion as well as  $V_{SM}$  ripple rise by reducing the second harmonic component of the circulating currents [10]. A balancing control algorithm (BCA) is applied to ensure the capacitor voltages to be balanced during normal operations [5].

## III. MTDC CONTROL

The strategies for the control of MTDC grids are summarized in this section. The traditional master and slave control is illustrated first, a detailed explanation of the P-Vdc droop control is depicted afterwards; a novel procedure for

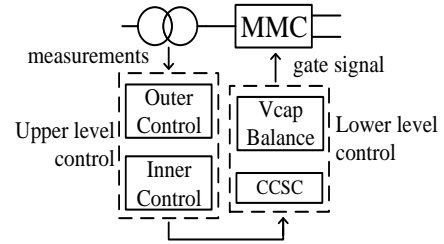


Fig.1: MMC control scheme.

incorporating multiple slack converters in the DC grid is described at the end.

### A. Constant Vdc Control (master and slave scheme)

In DC networks Vdc is the balancing signal, which has to be kept constant during normal operations. In “Constant Vdc Control” the master and slave approach is applied, the master (or slack) converter is in charge of controlling Vdc while the others control the active power transfers. The master adapts its power flow automatically to ensure the power balance within the DC grid [6]. Such a centralized control strategy requires the slack converter to react fast to transients, to be overrated and connected to a strong AC system [11], [12]. However, this strategy is not robust as it does not ensure grid reliability and stability in case of an outage of the master/slack station.

In order to regulate the power flow in the DC grid and maintain Vdc at the reference level, the voltage controller moderates  $i_{dref}$ , which is the input of the inner control current loop. The difference between Vdc measured and Vdc reference is processed through a PI controller to obtain the desired  $i_{dref}$ , as shown in Fig. 2a. The active power controller operates with a similar principle, as illustrated in Fig. 2b [13].

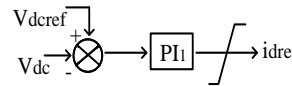


Fig.2a: Basic scheme for Vdc control.

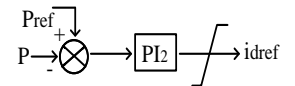


Fig. 2b: Basic scheme for P control.

### B. P-Vdc Droop Control (peer-to-peer scheme)

P-Vdc droop control method is applied in MTDC grids to facilitate the power sharing after a converter outage. This coordinated approach allows all the substations to participate to the power balancing, reducing the power mismatch the slack converter would compensate for in the “Constant Vdc Control” method. Since the presence of multiple slack converters would raise conflicts, the addition of droop to power controllers permits the regulation of power flows according to DC voltage variations. P-Vdc droop control principle is similar to the frequency droop control for AC systems; however Vdc is not a univocal value due to the voltage drops caused by the line resistances in the DC grid [6]. The implementation of P-Vdc droop suspends the requirement to have a master converter in the MTDC network [11]; this will ensure the correct power sharing in case of converter tripping at the cost of jeopardizing voltage stability, as Vdc may exceed the limits. The Vdc acceptable limits are a project

design specification, in common practice the voltage in a DC grid must be kept within +1.05 p.u. and -0.95 p.u..

The operating principle of P-Vdc droop control is described in Fig. 3. It aims to modify the power reference after a variation in Vdc, as a consequence of a contingency, is detected. The value of the droop constant  $\beta$  defines the sharing of the power imbalance between the terminals. Identical droop parameters would cause an equal power sharing between the all converters. If unequal values are selected, the larger ones will have a more significant contribution in the control loops [14]. In order to select the most convenient value for the droop  $\beta$  a sensitivity analysis is carried out; factors like converters rating and cable parameters (resistance) are considered to estimate which droop rate gives the best response in terms of voltage profile and sharing of power mismatch.

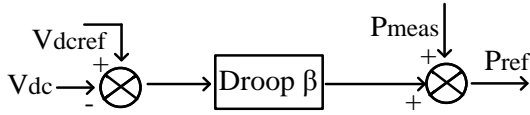


Fig.3: P-Vdc droop applied in P-Q controlled converters.

A detailed post contingency analysis for MTDC grid where converters are equipped with voltage droop control is offered in [14] and it will be briefly recalled hereafter. Naming  $P_i$  the real power output from the  $i^{\text{th}}$  converter,  $P_i^*$  the corresponding reference power and  $P_{loss}$  the total loss due to voltage drops along the DC lines, in steady state the system is described by (1), (2) and (3).

$$\sum_i P_i^* = 0, P_{loss} = - \sum_i P_i \quad (1) \text{ and } (2)$$

$$P_i = P_i^* + \frac{-P_{loss}}{\beta_i \sum_i (1/\beta_i)} \quad (3)$$

Equation (3) has been calculated through several algebraic passages and it includes the effect of the fixed value voltage droop ( $\beta$ ). After the outage of the  $n^{\text{th}}$  converter, the post contingency state (indicated by') is defined by (4).

$$P_i' = P_i^* + \left[ \frac{(-P_{loss}' + P_n^*)}{(\beta_i \sum_i^{n-1} 1/\beta_i)} \right] \quad (4)$$

Where  $P_n^* = \sum_i^{n-1} P_i^*$  and  $P_{loss}'$  is the total DC transmission loss after the fault. Assuming that all converters have the same rating and neglecting the DC power losses, a simplified expression for the power variation is given by (5). This underlines that after the outage of the  $n^{\text{th}}$  converter, the remaining  $n-1$  converters will share the power burden equally.

$$\Delta P_i = P_i' - P_i = \frac{P_n^*}{(n-1)} \quad (5)$$

### C. Master Droop Control (for Vdc-Q converters)

In normal conditions the presence of two slack converters in a MTDC grid may lead to conflicts. As mentioned earlier nor "Constant Vdc Control" neither "P-Vdc Droop Control" are able to guarantee grid reliability and voltage stability in high loading conditions if an outage occurs at the master

converter. The control strategy here described suggests the presence of two slacks to overcome the limitations of the previous control methods and to ensure a correct power sharing along with a stable voltage profile.

The coexistence of two Vdc-Q controlled converters is made possible through the variation of the Vdc reference signal in the Vdc control loop of the two slacks. As illustrated in Fig. 4, the reference voltage is modified via a droop considering the value of Idc, measured at the converter terminal. Idc is selected as it is directly subjected to variations after a converter outage occurs. The droop constant  $\gamma$  is tuned according to the operating conditions and the converter rating. The estimation of  $\gamma$  value is achieved through a sensitivity analysis approach. Strict constraints are applied to  $\gamma$ ; for  $\gamma < \gamma_{\min}$  the droop action is ineffective, for  $\gamma > \gamma_{\max}$  the deviation between the voltage references is too large preventing the system from maintaining stability. The application of a "Master Droop Control" allows a better voltage recovery in case of an outage in one of the slacks, as the other will keep Vdc within the acceptable limits.

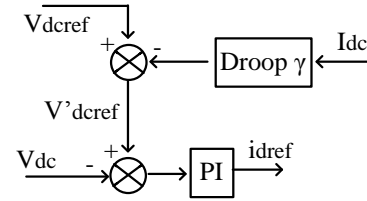


Fig.4: Modifications of Vdcref in Vdc-Q control of a slack converter.

## IV. CASE STUDY

A test network consisting of 5 symmetrical monopole converter stations has been developed in RT-Lab Simulator and it is shown in Fig. 6. The meshed topology is selected as it represents the structure of most future MTDC grids (North Sea, Zhoushan). The system includes both onshore grids and offshore wind farms: terminals #1, #2, #3, #5 are linked to AC systems represented by ideal voltage sources, whereas terminal #4 is connected to an offshore wind farm. Doubly Fed Induction Generators (DFIGs) are used to model the wind turbines. All the substations are equipped with the MMC based VSC-HVDC model described in Section II. The terminals are connected via 100 km long underground DC cables. The cables are designed as distributed parameters lines using OPAL Artemis model. The properties of the MTDC test grid are summarized in Table I and II.

In the study network, converter #1 is the master and it is controlled in Vdc-Q, converters #2, #3, #5 are regulated in P-Q. The wind farm controller regulates Vac and frequency to ensure that the maximum amount of power generated by the wind turbines is injected into the grid [15], [16]. Thanks to the capability of VSC to transmit power in either direction, every terminal behaves as rectifier or inverter according to the operating conditions. For this case study the power flows considered are shown in Fig. 5 (+ means injected power, - means exported power).

TABLE I. MTDC CHARACTERISTICS

AC side		DC side		DC cables	
V <sub>ac</sub>	220 kV	V <sub>dc</sub>	±320 kV	R	0.0127 Ω/km
P <sub>rated</sub>	1000MW	L <sub>dc</sub>	14mH	L	0.93 mH/km
SCR	20	R <sub>dc</sub>	3e7 Ω	C	12.74 nF/km

TABLE II. WIND TURBINES PROPERTIES

Offshore Wind (DFIG)			
P <sub>nom</sub> per unit	2.22 MW	V	575 V
N of unit	50	N <sub>nom</sub>	1500 rpm

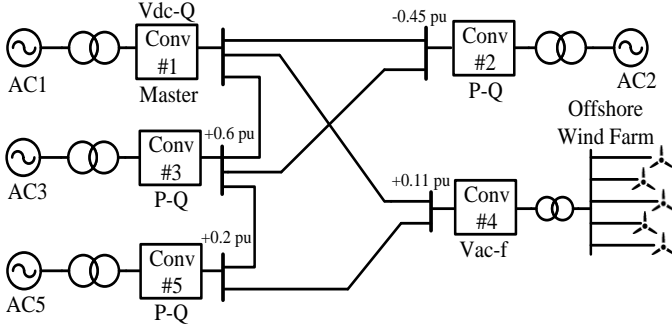


Fig. 5: 5-terminal DC grid model developed in RT-Lab Simulator.

## V. SIMULATIONS AND RESULTS

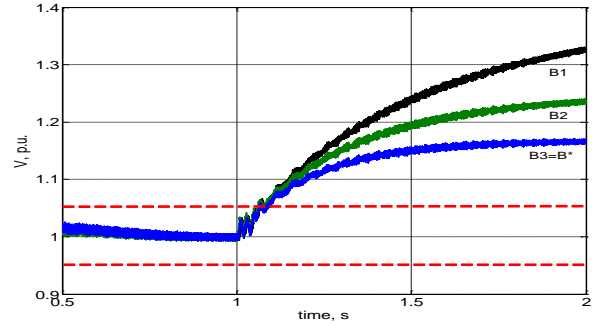
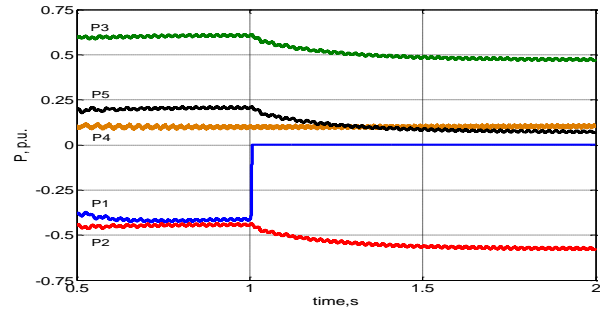
This section offers a representative set of time-domain simulations conducted in RT-Lab Simulator to assess the effectiveness of the MTDC control strategy proposed in Section III C. The evaluation of  $\beta$  and  $\gamma$  droop constants is defined through a sensitivity analysis approach. The power flows in steady state are as shown in Fig. 5. An outage on converter #1 at 1 s has been applied. The dynamic performance of the system has been analyzed considering two scenarios:

- Case1: Converter #1 is the only master in the MTDC grid. Converters #2, #3, #5 are regulated in P-Q and equipped with P-Vdc droop. Converter #4 is controlled in Vac-f.
- Case2: Converters #1 and #2 are both masters. Converters #3, #5 are regulated in P-Q and equipped with P-Vdc droop. Converter #4 is controlled in Vac-f.

### A. Case1: P-Vdc Droop Control

The dynamic response of the system has been examined considering the disconnection of converter #1. Several values of droop constant  $\beta$  have been tested and the voltage profiles are illustrated in Fig. 6a; the black, green and blue curves represent the voltage response of the MTDC grid for  $\beta_1=0.5$ ,  $\beta_2=0.8$  and  $\beta_3=1.2$  respectively. The values of  $\beta$  are chosen in the range  $\beta_{\min} < \beta < \beta_{\max}$ . For  $\beta < \beta_{\min}$  ( $=\beta_1$ ) the overall system stability is no longer preserved, variations in power flows are small, power mismatch takes long to be balanced and dc voltage is not kept within the nominal limits. For  $\beta > \beta_{\max}$  ( $=\beta_3$ ) the effect of the P-Vdc droop control becomes negligible. In pre-fault condition the voltage is kept at 1 p.u.; in the post-contingency state it is observed to rise above the Vdc acceptable limits (+1.05 p.u.; -0.95 p.u.) for every values of  $\beta$ .

It is noted that  $\beta_1$  case produces the worst response causing the voltage to increase up to 1.3 p.u. as  $\beta_1$  is too small. The selection of larger  $\beta$  droop constants ( $\beta_2$  and  $\beta_3$ ) generates more significant variations in the allocation of the power mismatch and it slightly improves the voltage profile reducing the rise to 1.25 p.u. (for  $\beta_2$ ) and 1.15 p.u. (for  $\beta_3$ ). Simulations show that  $\beta_3$  produces the best voltage profile, therefore the optimal value for the P-Vdc droop control is selected  $\beta^*=\beta_3$ . Fig. 6b shows the power sharing in the DC grid considering the P-Vdc droop constant  $\beta^*=\beta_3$ . After the outage occurs and P1 is reduced to 0 p.u., thanks to the action of P-Vdc droop control the power flows from converters #2, #3 and #5 are modulated in order to share the mismatch and keep the power balance within the grid ( $P_{in} = P_{out} + P_{loss}$ ). This set of dynamic tests underlines the constraints of the P-Vdc droop control method: it ensures the correct power sharing but it does not guarantee Vdc to stay within the limits.

Fig. 6a: Vdc in the DC grid for different values of  $\beta$ . Voltage limits (+1.05, -0.95) shown in red.Fig. 6b: Converter power flows for  $\beta=B^*$  (+ means injected power, - exported power).

### B. Case2: Multiple Master Converters

The modification of the Vdc reference signal in the voltage control loop of converters #1 and #2 allows the presence of two slacks in the MTDC grid. As Fig. 7a and 7b show, no conflicts are detected in steady state. At 1 s converter #1 trips and the dynamic performance of the MTDC in terms of Vdc and P is illustrated in Fig. 7a and Fig. 7b respectively. The selection of  $\gamma$  constant, which defines the master droop control, is evaluated via sensitivity analysis. Droop values have to be chosen in the range  $\gamma_{\min} < \gamma < \gamma_{\max}$ , where  $\gamma_{\min}=0.01$  and  $\gamma_{\max}=0.1$ . For  $\gamma < \gamma_{\min}$  the action of the master droop strategy is ineffective, for  $\gamma > \gamma_{\max}$  the deviation between the master voltage references is too large, hence the voltage profile rises above the acceptable limits and stability

is no longer ensured. Considering  $\beta=\beta^*$  for P-Vdc droop and selecting  $\gamma$  within the acceptable range,  $\gamma_1=\gamma_{\min}$  and  $\gamma_2=0.05$  are the constant values which produce the most adequate voltage profiles. Fig. 7a shows the voltage profiles for  $\gamma_{\min}$  (blue),  $\gamma_2$  (green) and  $\gamma_{\max}$  (black). Vdc is kept within the acceptable limits for  $\gamma_{\min}$  and  $\gamma_2$ , it rises up to 1.05 p.u. and then it promptly returns to its nominal value. The best voltage profile, near to 1p.u., can therefore be associated to any value between  $\gamma_{\min}$  and  $\gamma_2$ ; in this case  $\gamma_1$  is named  $\gamma^*$ . In Fig 7b the power sharing for  $\beta^*$  and  $\gamma^*$  is illustrated. It is influenced by the P-Vdc droop to a small extent, whose contribution is visible only in the transient immediately after the fault where P3 and P5 slightly decrease to balance the variation of P2. The second master (#2) mainly compensates for the power mismatch. The results demonstrate that the proposed control strategy guarantees a balanced power sharing along with fast DC voltage recovery.

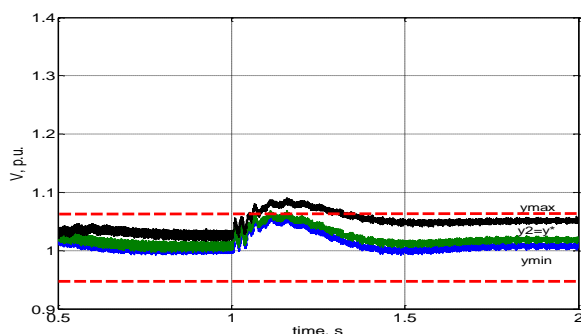


Fig. 7a: Vdc in the DC grid for different values of  $\beta$ . Voltage limits (+1.05, -0.95) shown in red.

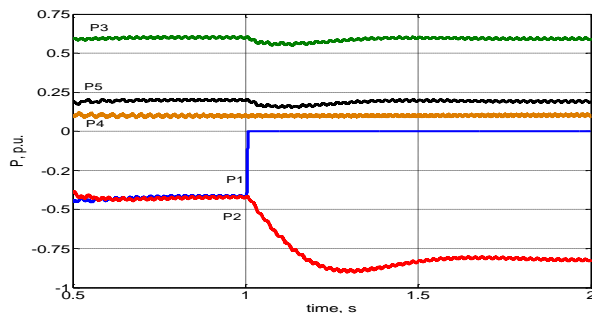


Fig. 7b: Converter power flows for  $\beta=\beta^*$  and  $\gamma=\gamma^*$  (+ means injected power, - exported power).

## VI. CONCLUSIONS

An alternative DC voltage control strategy that ensures the correct power sharing along with voltage stability in case of an outage in the slack converter has been proposed. It overcomes the limitations associated with the other control methods thanks to the coexistence of two master converters. The modification of the Vdc reference signal in their control loops prevents the rise of conflicts, which would appear normally in a MTDC with two converters in charge of controlling Vdc. To facilitate the testing of this control strategy a 5-terminal DC grid has been created in RT-Lab Simulator. The substations are equipped with MMC based VSC-HVDC model and they connect both onshore AC systems and offshore wind farms. With the increasing interest in MTDC, the development of an effective and robust

coordinated control strategy is of critical importance to ensure grid stability and reliability, in the perspective of incorporating these DC schemes within a bigger transmission system, such as the future European Super Grid.

## ACKNOWLEDGMENT

The authors gratefully acknowledge the support of the EPSRC (www.epsrc.ac.uk) for the financial support for Ms Spallarossa by the Top & Tail Transformation program grant (EP/I031707/1).

## REFERENCES

- [1] N. Ahmed, A. Haider, D. Van Hertem, Lidong Zhang and H.-. Nee, "Prospects and challenges of future HVDC SuperGrids with modular multilevel converters," in *Power Electronics and Applications (EPE 2011), Proceedings of the 2011-14th European Conference on*, 2011, pp. 1-10.
- [2] D. Van Hertem and M. Ghandhari, "Multi-terminal VSC HVDC for the european supergrid: Obstacles," *Renewable and Sustainable Energy Reviews*, vol. 14, no. 9, pp. 3156-3163, 12 2010.
- [3] Jing Hu, Chengyong Zhao, Xuena Zhang and Xiaodong Yang, "Simulation study of the Zhoushan project as a three-terminal DC transmission system," in *Power and Energy Society General Meeting, 2012 IEEE*, 2012, pp. 1-6.
- [4] P. Kundur, *Power System Stability and Control*, 6 ed., McGraw-Hill, 1994.
- [5] H. Saad, J. Peralta, S. Denetiere, J. Mahseredjian, J. Jatskevich, J.A. Martinez, A. Davoudi, M. Saeedifard, V. Sood, X. Wang, J. Cano and A. Mehrizi-Sani, "Dynamic averaged and simplified models for MMC-based HVDC transmission systems," *Power Delivery, IEEE Transactions on*, vol. 28, no. 3, pp. 1723-1730 2013.
- [6] T.M. Haileselassie and K. Uhlen, "Impact of DC line voltage drops on power flow of MTDC using droop control," *Power Systems, IEEE Transactions on*, vol. 27, no. 3, pp. 1441-1449 2012.
- [7] J. Peralta, H. Saad, S. Denetiere, J. Mahseredjian and S. Nguefeu, "Detailed and averaged models for a 401-level MMC-HVDC system," *Power Delivery, IEEE Transactions on*, vol. 27, no. 3, pp. 1501-1508 2012.
- [8] U.N. Gnanarathna, A.M. Gole and R.P. Jayasinghe, "Efficient modeling of modular multilevel HVDC converters (MMC) on electromagnetic transient simulation programs," *Power Delivery, IEEE Transactions on*, vol. 26, no. 1, pp. 316-324 2011.
- [9] J. Descloux, P. Rault, S. Nguefeu, J. Curis and X. Guillaud, "HVDC meshed grid: Control and protection of a multi-terminal HVDC system," in *Cigre 2012 Conference Proceeding*, Paris, France, 2012.
- [10] Qingrui Tu, Zheng Xu and Jing Zhang, "Circulating current suppressing controller in modular multilevel converter," in *IECON 2010 - 36th Annual Conference on IEEE Industrial Electronics Society*, 2010, pp. 3198-3202.
- [11] J. Beerten, D. Van Hertem and R. Belmans, "VSC MTDC systems with a distributed DC voltage control - A power flow approach," in *PowerTech, 2011 IEEE Trondheim*, 2011, pp. 1-6.
- [12] J. Beerten, S. Cole and R. Belmans, "Generalized steady-state VSC MTDC model for sequential AC/DC power flow algorithms," *Power Systems, IEEE Transactions on*, vol. 27, no. 2, pp. 821-829 2012.
- [13] F. Gonzalez-Longatt and J.M. Roldan, "Effects of dc voltage control strategies of voltage response on multi-terminal HVDC following a disturbance," in *Universities Power Engineering Conference (UPEC), 2012 47th International*, 2012, pp. 1-6.
- [14] N.R. Chaudhuri and B. Chaudhuri, "Adaptive droop control for effective power sharing in multi-terminal DC (MTDC) grids," *Power Systems, IEEE Transactions on*, vol. 28, no. 1, pp. 21-29 2013.
- [15] J. Cao, W. Du, H.F. Wang and S.Q. Bu, "Minimization of transmission loss in meshed AC/DC grids with VSC-MTDC networks," *Power Systems, IEEE Transactions on*, vol. 28, no. 3, pp. 3047-3055 2013.
- [16] B. Silva, C.L. Moreira and H. Leite, "Operation and control of multiterminal HVDC grids following the loss of an onshore converter," in *Innovative Smart Grid Technologies Latin America (ISGT LA), 2013 IEEE PES Conference On*, 2013, pp. 1-8.